NJC

Accepted Manuscript

This is an *Accepted Manuscript*, which has been through the Royal Society of Chemistry peer review process and has been accepted for publication.

Accepted Manuscripts are published online shortly after acceptance, before technical editing, formatting and proof reading. Using this free service, authors can make their results available to the community, in citable form, before we publish the edited article. We will replace this *Accepted Manuscript* with the edited and formatted *Advance Article* as soon as it is available.

You can find more information about *Accepted Manuscripts* in the Information for Authors.

Please note that technical editing may introduce minor changes to the text and/or graphics, which may alter content. The journal's standard Terms & Conditions and the Ethical guidelines still apply. In no event shall the Royal Society of Chemistry be held responsible for any errors or omissions in this *Accepted Manuscript* or any consequences arising from the use of any information it contains.

ROYAL SOCIETY OF CHEMISTRY

www.rsc.org/njc

A sol-gel way to synthesize SiO_2/TiO_2 well nanocrystalline mesoporous photocatalyst through ionic liquid controlling

Fengfeng Zhang, Dayin Sun, Chunling Yu, Yuxin Yin, Hongyi Dai* and Guolin Shao*

Corresponding author: Prof. DAI Hongyi, daihongyi@dlpu.edu.cn

(School of Light Industry and Chemical Engineering, Dalian Polytechnic University, Liaoning Dalian 116034)

Abstract: SiO_2 composited TiO_2 photocatalysts were prepared through a sol-gel way, ionic liquid (IL), 1-butyl-3-methylimidazole bromide ([Bmim]Br), used as a structure controlling agent. The obtained materials were characterized by Fourier transform (FT-IR) spectroscopy, powder X-ray diffraction (XRD), N_2 adsorptione-desorption isotherms, scanning electron microscopy (SEM) and transmission electron micrographs (TEM). The as-prepared TiO_2 nanoparticles present anatase crystal phase even without being calcined, and show better photocatalytic performance in the degradation of reactive brilliant blue. The results showed that a suitable aging concentration of IL was beneficial to the growth of crystalline particles, but harmful more than the limit. Micelle State Charge Field (MSCF) leading to lyotropic liquid crystalline mesophases was first presented to describe the action of IL in the formation of crystals and porosities.

Keywords: SiO_2/TiO_2; ionic liquid; sol-gel; anatase; nanocrystalline; micelle state charge field (MSCF)

1. Introduction

Compared to the conventional organic solvents, the ionic liquids (ILs) can be used as template, solvent and reactor in the synthesis of inorganic materials for its unique properties such as extremely low volatility, high ionic conductivity, good dissolving ability, designable structures, nontoxicity, and a large electrochemical window. Many reports have described ILs as catalysts in organic reactions or polymerizations. Recently, there have been growing interests in inorganic porous material preparation using ILs as templates, such as synthesis of a molecular sieve or aerogel [1]. Due to the generally negligible vapor pressure of ILs, it has been suggested that ILs could be used as non-volatile drying control chemical additives (DCCAs) during the synthesis of sol-gels, resulting in reduced shrinkage and subsequent matrix collapse during formation of the gels [2].

TiO_2, regarded as the most efficient environmental semiconductor photocatalyst, has been widely studied. Admittedly, the principle of photocatalysis is absorption of photons with energy larger than the band gap of TiO_2 and electrons are excited from the valence band to the conduction band, creating electron-hole pairs [3]. The photocatalytic activity of a semiconductor is largely controlled by the light absorption properties, reactive rates on the surface by the electron and hole, and the electron-hole recombination rate. The formed photogenerated electron-hole pairs can react in three possible pathways as illustrated in Scheme 1. Larger surface area and slower recombination lead to faster photocatalytic reaction [4]. Contradictorily, the surface is a defective site, therefore, larger surface area leads to faster recombination. Higher crystallization with fewer bulk defects is beneficial to photocatalytic activity. There are three main crystal phases in titania materials, rutile, anatase and brookite, among which, crystalline anatase was investigated frequently because of its photocatalytic activities for various applications [5, 6]. So that, how to synthesize a catalyst with high surface area and anatase microcrystal is the common goal for researchers [7, 8]. A traditional route to improve the crystallinity of titania material is high temperature treatment. What crystal formed depends on the condition of synthesis. Rutile is the thermodynamic stable phase, but anatase or brookite is stable at small particle size and lower

temperature [9]. High temperature treatment can induce aggregation of small nanoparticles, decrease of surface area and collapse of porous structure. Many efforts have been performed to solve this problem [10, 11]. Researchers used different surfactants as structure-directing agents or template agents to synthesize mesoporous titania, successfully acquired higher surface area and pore volume, but the titania were amorphous with poor photocatalystic activity [12]. In particular for the systems doped SiO_2, silica provided stability, mechanical strength and acid sites, which is beneficial to application and recycle usage of catalyst [13-15].

The sol-gel method is a versatile process of making various porous materials and is widely used to synthesize titania or silica doped titania photocatalyst [16-18]. A typical sol-gel process includes follow steps: hydrolysis and polymerization of colloidal suspension or solution of precursores such as metal alkoxides, aging of polymers to form porous and net skelecton structure, extraction of solvent and dry to solidify gel phase. As a result, the dry samples keep the very unusual porous texture that they had in the wet stage. In general, these dry solids have very low apparent densities, large specific surface areas, and in most cases, they exhibit amorphous structures when examined by X-ray diffraction (XRD) methods [17]. A highly porous and extremely low-density material called an aerogel is usually obtained under a supercritical condition, which is employed to prevent the porous structure from collapsing during drying. Among them, the silica aerogel have been widely reported. One way to enhance the titania-specific surface area is dispersing titania into a silica matrix. The sol-gel process was proven to be convenience method for the formation of homogeneous bulk silica-titania structure by controlling hydrolysis and condensation of silica and titania precursors to form Si-O-Ti bonding [19, 20].

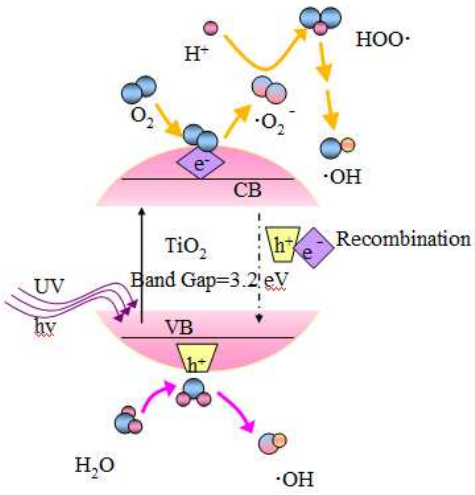

Scheme 1. The schematic of photocatalytic mechanism in UV

We have reported a sol-gel route of synthesizing silica aerogel under ambient pressure drying through IL controlling. The aerogels were bulk with high surface area ($992 m^2/g$), mesoporous structure and narrow pore size distribution [1]. Similar method was used to synthesize photocatalysts. Interestingly, we found that under IL controlling, mesoporous bulk titania or titania/silica composite with well anatase nanocrystalline structure can been synthesized at low temperature (aging at 60 °C) without calcination, but excessive ionic liquid can make the product formation of amorphous, which rare reported in literature. In this paper, we demonstrate the effect of IL ([Bmim]Br) as aging solution on the formation of crystal. The reasons of forming crystalline mesoporous structure have been discussed.

2. Experimental

2.1 Materials

Tetraethyl orthosilicate (TEOS, P 98%) and butyl titanate (TBT, P 97%) were obtained from Dongtai Tianjin Kemiou Chemical Reagent Co., used as titania and silica precursor, respectively. Ethanol (≥99.7%, Tianjin Guangfu Fine Chemical Research Institute); Acetic acid (Tianjin Jindong Tianzheng Fine Chemical Reagent Factory); Urea (Shenyang reagent five factory); Cyclohexane (Tianjin Kermel Chemical Reagent Co. Ltd., China), all of these were analytical grade. Reactive brilliant blue (Ji'nan Longteng dye Chemical Co. Ltd China.) used for the photocatalytic activity tests . The [Bmim]Br, 1-butyl-3-methylimidazole bromide was synthesized according to the method reported in the literature [21].

2.2 Preparation of photocatalysts

Mesoporous TiO_2 and SiO_2/TiO_2 mixed oxides were prepared via a sol-gel route. At first, the silica sol was prepared by adding solution (EtOH : H_2O : acetic acid : urea : IL molar ratio was 3.5 : 4.62 : 0.002 : 0.04 : 1, stirred for 15 minutes at room temperature) to a tetraethylorthosilicate in ethanol solution (TEOS/EtOH molar ratio was 1 : 3.5, stirred for 15 minutes at room temperature), and the mixture solution was stirred for 1.5 h at room temperature. The final molar ratio of TEOS : EtOH : H_2O : Acetic acid : Urea : IL molar ratio was 1 : 7 : 4.62 : 0.002 : 0.04 : 1. Then the TiO_2 sols was prepared by adding solution (EtOH : H_2O : Acetic acid : Urea : IL molar ratio was 9 : 3.75 : 1.8 : 0.04 : 1, stirred for 15 minutes at room temperature) to a butyl titanate in ethanol solution (TBT/EtOH molar ratio was 1 : 9, stirred for 15 minutes at room temperature), and the mixture solution was stirred for 30 minutes at room temperature. The final molar ratio of TBT : EtOH : H_2O : Acetic acid : Urea : IL molar ratio was 1 : 18 : 3.75 : 1.8 : 0.04 : 1. The mix sol was directly mixed TiO_2 sol with SiO_2 sol under vigorous stirring at TiO_2/SiO_2 molar ratios 10, after 30 minutes of stirring then the prepared sol placed in a water bath (30 °C) in the atmospheric for three days, Then add different concentrations of ionic liquids, and aging for 4 days in a water bath (60 °C) to prepare a series of TiO_2/SiO_2 mixed oxide photocatalysts samples. The IL in the gels was extracted with cyclohexane and alcohol in turn until Br^- ion cannot be detected by silver nitrate, and then, dried at 60 °C for 8 h at ambient pressure.

2.3 Characterization

The Brunauer-Emmett-Teller (BET) surface area and the porosity of the samples were studied by a nitrogen adsorption instrument (Nova 1200e Surface Area and Pore Size Analyzer). All the samples measured were degassed at 150 °C for 2 h prior to actual analysis. Pore size distribution and specific desorption pore volumes were obtained using by the Barrett-Joyner-Halenda (BJH) method. X-Ray diffraction analysis (XRD) was performed using by a D/max-3B Analyzer (Cu-Kα, 40 kV, 30 mA). The morphology of samples were investigated by scanning electron microscopy (SEM) (Hitachi S-2500). FT-IR spectroscopy (PerkinElmer, Spectrum One-B) was used to determine the bonding of silica-titania composite. Samples for transmission electron microscopy (TEM) were prepared by placing a droplet of the suspension of photocatalysts onto a copper grid and allowing the solvent to evaporate. The high-resolution transmission electron microscopy (HRTEM) images were obtained on a FEI TECNAI G2 F20 microscope at an accelerating voltage of 200 kV.

2.4 Photocatalytic performance

The photocatalytic performance of the samples was evaluated by decolorization of reactive brilliant blue (KN-R). The 0.1 g block samples were used to decolorize 400 ml reactive brilliant blue solution (40 mg/L). The photocatalytic

reaction was performed under 135 W Xenon lamp irradiation. In the first 30 minutes, the reaction was performed in darkness, after 30 minutes, 135W xenon lamp irradiation for 2 hours, and observe the UV-Vis absorbance spectra of each sample.

3. Results and discussion

3.1. Catalysts characterization

3.1.1 XRD analysis

The silica composited titania possessed fine nano-crystalline anatase phase similar as mesoporous titania based on the investigation of XRD shown in Fig.1. Usually, the porous material synthesized by sol-gel method was amorphous without calcinations [3, 4]. Obviously, the IL played an important role on the formation of crystalline phases. Further investigations showed the concentrations of IL, [Bmim]Br, evidently effected on the crystallization for both sol and gelatin step, especially for later step. To clarify the effect of IL, we used different concentration of IL as aging solution to prepare a series of SiO_2/TiO_2 mixed oxide photocatalysts samples. The XRD pattern of the pure TiO_2 showed crystalline structure of the pure anatase phase, main diffraction peaks near or at the diffraction angle for 25.3°, 37.8°, 48.1°, 53.9°, 62.7°, 68.8° and 75.0° can be observed, corresponding to (101), (004), (200), (105), (204), (116) and (215) plane diffraction of anatase, respectively. SiO_2 composited TiO_2 photocatalysts with IL concentrations of 0 mol/L, 1 mol/L and 2 mol/L also showed diffraction peaks attributed to the anatase TiO_2, the incorporated SiO_2 did not affect the crystalline structure of the TiO_2. The changes of XRD patterns clearly showed that a suitable aging concentration of IL was beneficial to the growth of crystalline particles, but harmful more than the limit. Based on the calculation of Scherrer equation of $D=0.89\lambda/\beta\cos\theta$, the crystal diameters were calculated from the (101) plane and changed from 2.0 nm, 6.6 nm, to 5.3 nm with the increasing the concentration of IL from 0 mol/L, 1 mol/L to 2 mol/L, because a further increase in the IL concentration more greatly inhibited the crystallization process of the TiO_2. When the concentration of IL reached or exceeded 3 mol/L, the peaks of XRD weakened and disappeared. Measured by conductance method in this paper, the critical micelle concentration (CMC) of ionic liquids was 0.84 mol/L. Viscosity increased with the concentration of ionic liquids from small to large, when the concentration of ionic liquid reaches 4 mol/L, viscosity is as high as 69.3 $g\cdot cm^{-1}\cdot s^{-1}$ and 15.2 $g\cdot cm^{-1}\cdot s^{-1}$, which were measured with viscosity meter at the temperature of 25 °C and 60 °C, respectively. The crystal shape of aging liquid at 1 mol/L was the best because of nanoparticles with a charge of sol. When the concentration of ionic liquid reached the critical micelle concentration, it would form micelles from the ion states, the interactions between ionic liquids micelle and TiO_2 nanoparticles made the nanoparticles orderly arranged and formed crystalline structure. The peaks of XRD weakened at the aging concentration of 0 mol/L, maybe in the process of sol configuration, it also contained a small amount of ionic liquid play a role in the ageing process and at the ionic liquid concentration was low to meet the critical micelle concentration. The peaks of XRD disappeared at the aging concentration of 3 mol/L may be due to the high viscosity of the aging , nanoparticles could not adequately spread and orderly arranged.

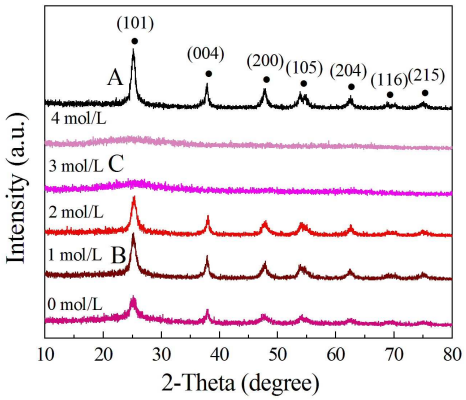

Fig.1. XRD patterns of pure TiO_2 and SiO_2/TiO_2 using different concentration of IL as aging liquid (0, 1, 2, 3, 4 mol/L)

A possible crystallization mechanism of titania was that the state charge field of IL micelles (called MSCF) leaded to well-ordered prepolymers, lyotropic liquid crystalline mesophases, and at last formed crystallites as pore walls. Because anatase is the thermodynamic stable phase at low temperature and small crystal diameter, the crystallite is simplex anatase phase. This process can be illustrated as Scheme 2. Because of nanoparticles with a charge of sol, When the concentration of ionic liquid reached the critical micelle concentration would form micelles from the ion states, interactions between ionic liquids micelle and nanoparticles made the nanoparticles orderly arranged to form crystalline structure. If the IL concentration is increased over the limit, the diffusion of prepolymers will become less available for high viscosity of medium; as a result, the crystallites cannot form. The MSCF seems difficult to answer questions from the conventional cation surfactants, which usually used as templates in sol-gel method, but have seldom been found the function as ILs in this work. It can be contributed to the imidazole cycle of IL, which as a catalyst accelerated the hydrolysis and condensation of titania or silica precursors, and simultaneously, itself was easily self-assembled by π-π stack [22] .

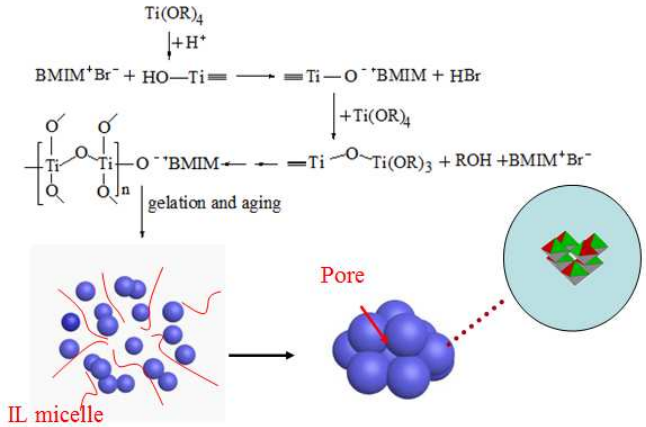

Scheme 2. The proposed mechanism for the formation of crystallite and porosity under the control of IL

3.1.2 N_2 adsorption-desorption analysis

The adsorption-desorption isotherms and pore size distribution for both catalysts were shown in Fig.2. The N_2

adsorption-desorption isotherm shape derived for the aerogels were identified as type-IV, with a capillary condensation at the pressure about p/p_0=0.4. The hysteresis loop for sample A can be classified as type H2 according to IUPAC classification [23]. Type H2 means porous structure as bottle shape, which is attributed to the holes left by IL micelles. The narrow pore size distribution of A was reasonable evidence. Differently, sample B should be classified as type H3, which meaned cylindrical shape hole or slit shape hole. Two peaks of the most probable pore size distributed at 3.86 nm and 7.92 nm imply two type holes in sample B, conjecturally derived from titian and silica [24]. The surface area, pore radius and pore volume of Sample A, B, C were shown in Table 1. The changes of TiO_2 stack structure because of doping silica can remarkably enhance the structure performance of catalysts, such as the increase of surface area and pore volume of sample B to 585 m^2/g and 0.913 mL/g, respectively. These values were much higher than for pure titanium (216 m^2/g, 0.343 mL/g), due to the microenvironment changes, two peaks all shifted to small diameters comparing with pure titania (6.3 nm) and silica (>20 nm). Obviously hysteresis loop for Sample A and Sample B may be the concentration of ionic liquid at 1mol/L would form micelles from the molecular states, micellar induced nanoparticles formed an orderly arrangement channel structure. No hysteresis loop for the sample C, which meaned that the sample concentration of ionic liquid too higher to effectively induced , disorderly accumulation without pore structure, which was in good agreement with the XRD results (Fig.1).

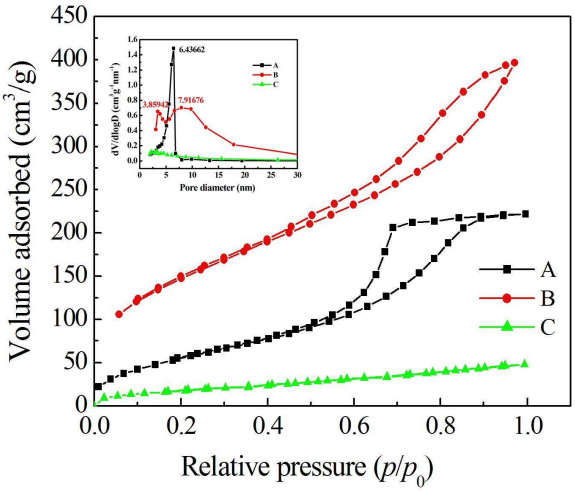

Fig.2. N_2 adsorption/desorption isotherms and pore size distributions of sample A (Pure TiO_2, IL, 1 mol/L), B (SiO_2/TiO_2, IL, 1 mol/L) and C (SiO_2/TiO_2, IL, 3 mol/L)

Table 1. The surface area, pore radius and pore volume of Sample A (Pure TiO_2, IL, 1 mol/L), B (SiO_2/TiO_2, IL, 1 mol/L), C (SiO_2/TiO_2, IL, 3 mol/L)

Photocatalyst	Surface area ($m^2 \cdot g^{-1}$)	Pore radius (nm)	Pore volume ($m^3 \cdot g^{-1}$)
Sample A	216.3	6.3	0.343
Sample B	585.2	4.4	0.913
Sample C	67.6	2.2	0.083

3.1.3 SEM analysis

The SEM images were shown in Fig.3. The appearance morphology of B was more similar with silica aerogel [1]. The particle size estimated by SEM roughly agreed with the results of XRD Scherrer calculation. No significant difference

could be seen between the two samples. The binary oxide catalyst was more uneven compared with sample A and no separated phase can be observed.

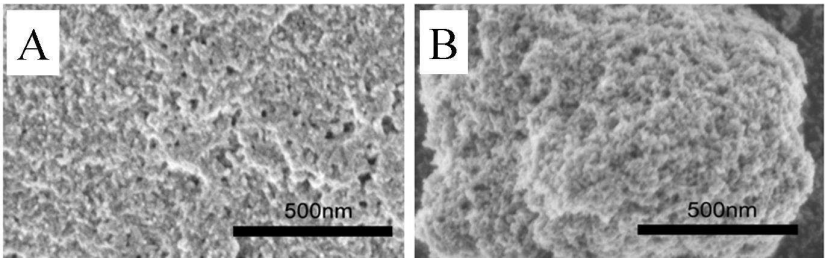

Fig.3. SEM images of sample A (Pure TiO_2, IL, 1 mol/L) and B (SiO_2/TiO_2, IL, 1 mol/L)

Fig.4 showed the element content distribution of Si and Ti. The silicon content was mostly constant within the measuring range. However, the titanium content changeed significantly. Results also showed that silica was uniformly distributed in bulk phase while the titania were in the formation of nanocrystal particles.

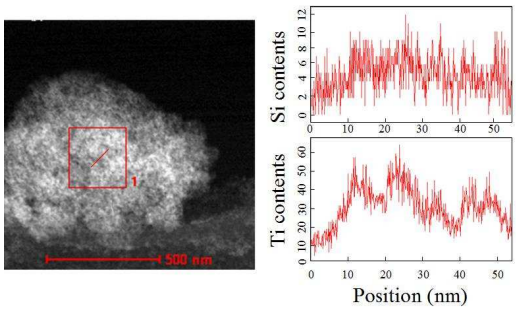

Fig.4. Si-element and Ti-element content distribution of sample B (SiO_2/TiO_2, IL, 1 mol/L) along the diagonal line in region 1

3.1.4 TEM analysis

The morphology of sample A (Pure TiO_2, IL, 1 mol/L) and B (SiO_2/TiO_2, IL, 1 mol/L) was further investigated by TEM. A1 and A2 are different magnifications for the sample A, A1 (Low-magnification), A2 (high-magnification). B1 and B2 are different magnifications for the sample B, B1 (Low-magnification), B2 (high-magnification). As shown in Fig.5 (A2) and Fig.5 (B2), two-dimensional lattice fringes can be observed via detailed high-resolution TEM tilted angle analysis. As shown in Fig.5 (A1), titania in spindle structure and grain grew completely, but the dispersion of TiO_2 nanoparticles was not uniform and prone to reunite. Fig.5 (B1), the growth of grains was restrained and weaken the spindle structure, grain width, but the dispersion of particles was relatively uniform, which was in good agreement with the XRD results (Fig.1). The following could be the cause of producing this kind of phenomenon:The external of titania coated with silica, inhibited the growth of the grains, crystallinity decreased.

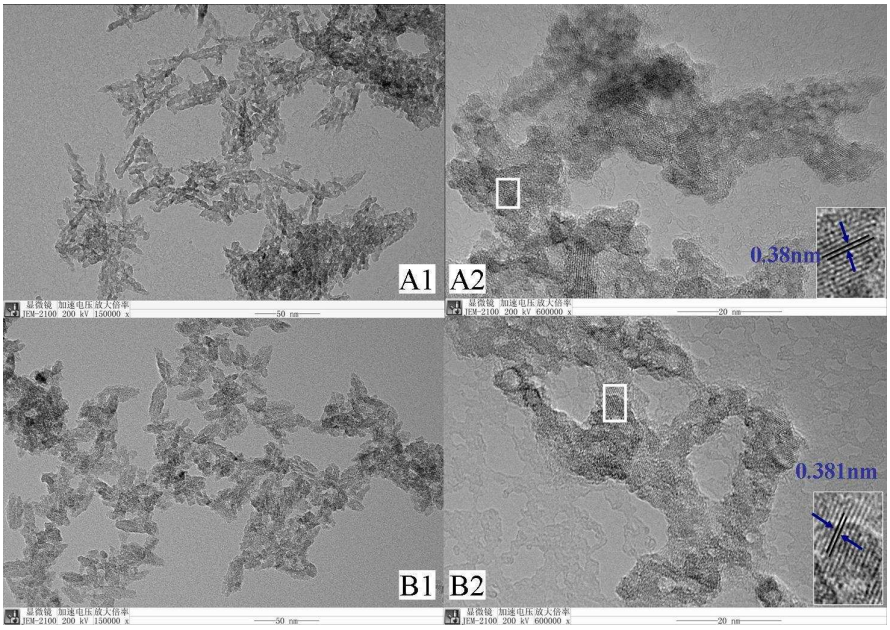

Fig.5. Transmission electron microscopy (TEM) images of A (TiO_2, IL, 1 mol/L) and sample B (SiO_2/TiO_2, IL, 1 mol/L), (A1, B1) Low-magnification and (A2, B2) high-magnification

3.1.5 FT-IR analysis

To show a more evidence on the combination of two dioxides, the FT-IR spectrum of B was shown in Fig.6 (B). Compared with pure titania, the big adsorption peak at 1087 cm^{-1} of Fig.6 (A) disappeared in curve B. A rational conjecture was the formation of Ti-O-Si bond by the insertion silica in titania network to enhance the titania-specific surface area was dispersing titania into a silica matrix, which was in good agreement with the BET results (Table 1).The characteristic peaks of Ti-O-Si bond appear at 1039 and 910 cm^{-1}, which were attributed to symmetric and anti-symmetric stretching of Ti-O-Si bond, respectively [19, 25]. The peak areas of broad band at 3400 cm^{-1} and band at 1630cm^{-1}, which respectively corresponded to the stretching of -OH and the deformation of H-O-H, increased from A to B, suggested water adsorbed on silica surface. It was generally accepted that water adsorbed on silica surface due to the formation of hydrogen bonding silinol [14]. The results further evidenced the inference that a part surface of hole wall was occupied by silica. The bridge bonds existed between the hole walls of crystalline titania and amorphous silica, which agreed with the results of Luís Pinho [24].

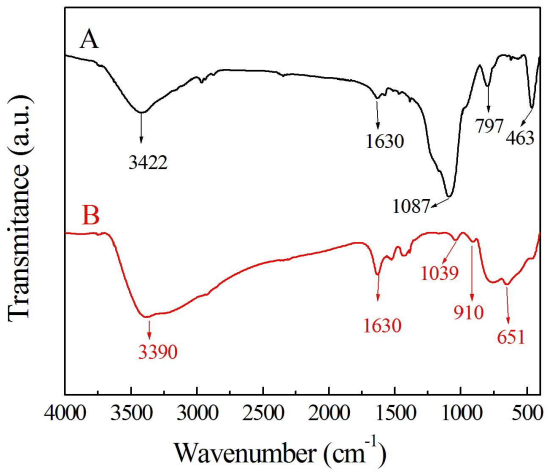

Fig.6. The FT-IR spectra of sample A (TiO_2, IL, 1 mol/L) and B (SiO_2/TiO_2, IL, 1 mol/L)

3.2 Photocatalytic performance

The 0.1 g block samples were used to decolorize 400 ml reactive brilliant blue solution (40 mg/L). The photocatalytic reaction was performed under 135 W Xenon lamp irradiation. In the first 30 minutes, the reaction was performed in darkness, after 30 minutes, 135W xenon lamp irradiation for 2 hours, and observe the UV-Vis absorbance spectra of each sample. Fig.7 showed the UV–vis spectra of reactive brilliant blue solution after 2 hours photo-degradation experiment with pure TiO_2 (IL, 1 mol/L,), SiO_2/TiO_2 (IL, 0 mol/L), SiO_2/TiO_2 (IL, 1 mol/L), SiO_2/TiO_2 (IL, 2 mol/L), SiO_2/TiO_2 (IL, 3 mol/L) as photocatalyst, 135W xenon lamp as light source, at room temperature and pressure, correspond to Fig.7(a), Fig.7(b), Fig.7(c), Fig.7(d), Fig.7(e), respectively. Fig.7(f) as the arrows in order from top to bottom on behalf of reactive brilliant blue without catalyst, SiO_2/TiO_2 (IL, 3 mol/L), pure TiO_2 (IL, 1 mol/L), SiO_2/TiO_2 (IL, 0 mol/L), SiO_2/TiO_2 (IL, 2 mol/L), SiO_2/TiO_2 (IL, 1 mol/L) in under xenon lamp irradiation for 2 hours after the catalytic degradation of reactive brilliant blue and UV visible absorption curve, obvious the photocatalytic activity of SiO_2/TiO_2 (IL, 1 mol/L) was much better than that of other Samples. Doping silica enhanced the photocatalytic performance of titania, because that it greatly improved the surface area. The reason should be that the titania-specific surface area was dispersing titania into a silica matrix, which was in good agreement with the BET (Table 1) and the FT-IR (Fig.6) results. Obviously, the IL plays an important role for the photo-degradation of reactive brilliant blue.

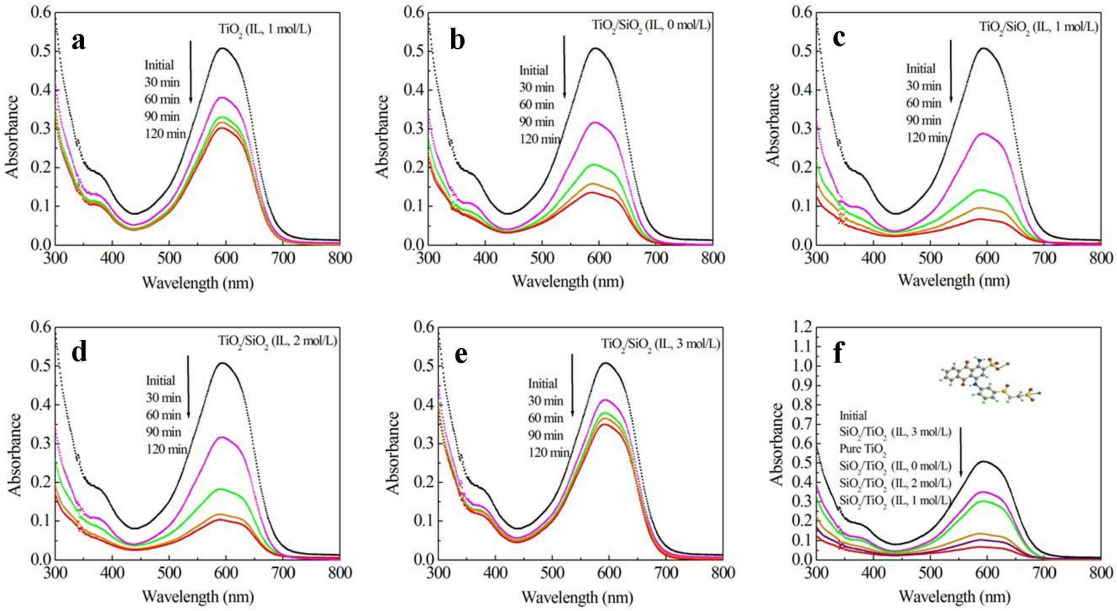

Fig.7. UV–vis spectra of reactive brilliant blue solution photo-degradation experiment with a (pure TiO_2, IL, 1 mol/L), b (SiO_2/TiO_2, IL, 0 mol/L), c (SiO_2/TiO_2, IL, 1 mol/L), d (SiO_2/TiO_2, IL, 2 mol/L), e (SiO_2/TiO_2, IL, 3 mol/L), and f (absorbance of all the samples after 2 hours) under xenon lamp irradiation.

4. Conclusions

SiO_2/TiO_2 mesoporous photocatalyst with nanocrystalline anatase and high surface area were successfully prepared with [Bmim]Br and sol-gel route under ambient pressure drying without calcinations. The results demonstrated that the lonic liquids had prominence effect on the formation of TiO_2 crystallites. Suitable concentration of lonic liquids for sol-gel process was required and beneficial to the growth of crystallite particles. In the process, crystalline titania and amorphous silica skeletons can be fabricated and banded together by the bond of Ti-O-Si. When the concentration of IL was 1 mol/L, SiO_2/TiO_2 composite aerogels was anatase, specific surface area up to 585.2 $m^2 \cdot g^{-1}$, and photocatalytic degradation of reactive brilliant blue was much better than that of other Samples. The Micelle State Charge Field (MSCF) should be the main factor leading to crystallization of TiO_2. Such a method and theory will facilitate the synthesis of photocatalysts and porous materials.

Acknowledgement

Supported from the Foundation of Liaoning Educational Committee (No. L2013220).

References

[1] H.Y. Dai, H.R. Yan, C.L. Yu, Y.H. Fu, G.L. Shao, L.Y. Ning, X.Y. Wu. *Adv. Mater. Res.*, 2013, 616-618, 1864-1868.

[2] M.A. Klingshirn, S.K. Spear, J.D. Holbrey, R.D. Rogers. *J. Mater. Chem.*, 2005, 15, 5174-5180.

[3] X.B. Chen, S.S. Mao. *Chem. Rev.*, 2007, 107, 2891-2959.

[4] A. Kubacka, M. Fernández-García, G. Colón. *Chem. Rev.*, 2012, 112, 1555-1614.

[5] C.S. Kim, J.W. Shin, S.H. An, H.D. Jang, T.O. Kim. *Chem. Eng. J.*, 2012, 204-206, 40-47.

[6] T. Nanba, S. Masukawa, J. Uchisawa, A. Obuchi. *Appl. Catal. A.*, 2012, 419-420, 49-52.

[7] D. Fattakhova-Rohlfing, J.M. Szeifert, Q. Yu, V. Kalousek, J. Rathouský, T. Bein. *Chem. Mater.*, 2009, 21, 2410-2417.

[8] K. Zimny, T. Roques-Carmes, C. Carteret, M.J. Stébé, J.L. Blin. *J. Phys. Chem. C.*, 2012, 116, 6585-6594.

[9] M.R. Ranade, A. Navrotsky, H.Z. Zhang, J.F. Banfield, S.H. Elder, A. Zaban, P.H. Borse, S.K. Kulkarni, G.S. Doran and H.J. Whitfield. J. *Proc. Natl. Acad. Sci.*, 2002, 99, 6476-6481.

[10] E. Beyers, P. Cool, E.F. Vansant. *J. Phys. Chem. B.*, 2005, 109, 10081-10086.

[11] D.W. Lee, S.J. Park, S.K. Ihm, K.H. Lee. *Chem. Mater.*, 2007, 19, 937-941.

[12] H. Shibata, T. Ogura, T. Mukai, T. Ohkubo, H. Sakai, M. Abe. *J. Am. Chem. Soc.*, 2005, 127, 16396-16397.

[13] S.V. Ingale, P.B. Wagh, A.K. Tripathi, A.S. Dudwadkar, S.S. Gamre, P.T. Rao, I.K. Singh, Satish C. Gupta J. *Sol-Gel Sci. Technol.*, 2011, 58, 682-688.

[14] U.K. Nizar, J. Efendi, L. Yuliati, D. Gustiono, H. Nur. *Chem. Eng. J.*, 2013, 222, 23-31.

[15] G. Calleja, D.P. Serrano, R. Sanz, P. Pizarro. *Microporous Mesoporous Mater.*, 2008, 111, 429-440.

[16] A. Karout, A.C. Pierre. *Catal. Commun.*, 2009, 10, 359-361.

[17] A.C. Pierre, G.M. Pajonk. *Chem. Rev.*, 2002, 102, 4243-4265.

[18] K.S. Yoo, T.G. Lee, J. Kim. *Microporous Mesoporous Mater.*, 2005, 84, 211-217.

[19] G.N. Shao, A. Hilonga, S.J. Jeon, J.E. Lee, G. Elineema ,D.V. Quang, J.K. Kim, H.T. Kim. *Powder Technol.*, 2013, 233, 123-130.

[20] Y. Horiuchi, H. Ura, T. Kamegawa, K. Mori, H. Yamashita. *J. Phys. Chem. C.*, 2011, 115, 15410-15415.

[21] J.G. Huddleston, A.E. Visser, W.M. Reichert, H.D. Willauer, G.A. Broker, R.D. Rogers. *Green Chem.*, 2001, 3, 156-164.

[22] Y. Zhou, J.H. Schattka, M. Antonietti. *Nano Lett.*, 2004, 4, 477-481.

[23] F. Rouquerol, J. Rouquerol, K. Sing. *Academic press, London*, 1999, vol. 11, pp. 191.

[24] L. Pinho, J.C. Hernández-Garrido, J.J. Calvino, M.J. Mosquera. *Phys. Chem. Chem. Phys.*, 2013, 15, 2800-2808.

[25] L. Zhao, D.X. Wang, J.S. Gao, C.M. Xu. *Chin. J. Catal.*, 2005, 26, 15-19.